# Copper-mediated dimerization of CopZ, a predicted copper chaperone from *Bacillus subtilis*

Margaret A. KIHLKEN*, Andrew P. LEECH† and Nick E. LE BRUN*[1]

*Centre for Metalloprotein Spectroscopy and Biology, School of Chemical Sciences and Pharmacy, University of East Anglia, Norwich NR4 7TJ, U.K., and †Bioanalytical Laboratory, School of Biological Sciences, University of East Anglia, Norwich NR4 7TJ, U.K.

Understanding the metal-binding properties and solution states of metallo-chaperones is a key step in understanding how they function in metal ion transfer. Using spectroscopic, bioanalytical and biochemical methods, we have investigated the copper-binding properties and association states of the putative copper chaperone of *Bacillus subtilis*, CopZ, and a variant of the protein lacking the two cysteine residues of the MXCXXC copper-binding motif. We show that copper-free CopZ exists as a monomer, but that addition of copper(I) causes the protein to associate into homodimers. The nature of the copper(I)–CopZ complex is dependent on the level of copper loading, and we report the detection of three distinct forms, containing 0.5, 1.0 and 1.5 copper(I) ions per protein. The presence of excess dithiothreitol has a significant effect on copper(I) binding to CopZ, such that, in its presence, copper(I)–CopZ occurs mainly as a monomer species. Data for copper binding to the double-cysteine variant of CopZ are consistent with an essential role for these residues in tight copper binding in the wild-type protein. We conclude that the complex nature of copper(I) binding to CopZ may underpin mechanisms of protein-to-protein copper(I) transfer.

Key words: Atx1, copper binding, copper metabolism.

## INTRODUCTION

Copper plays an essential role in proteins involved in many important cellular processes [1]. At the same time, it is also potentially extremely toxic, for example via catalysis of the formation of highly reactive radical species [2]. Thus an organism must be able to control the form and concentration of intracellular copper. How this is achieved is a topic of intense current interest, and it is becoming clear that cells maximize the benefits and minimize the toxicity of this metal ion by keeping it tightly bound to proteins [3–6]. The assembly of copper-containing proteins, therefore, requires specific protein factors, called copper chaperones because they direct copper in a highly specific manner to their target proteins. Via chaperones, mobile copper is tightly bound within a cell and consequently unable to participate in potentially deleterious chemical reactions.

In order to understand how copper chaperones carry out their function, it is necessary to understand how they bind copper, e.g. which residues are directly and indirectly involved, and details of the thermodynamics of binding and binding stoichiometries. Structural studies by NMR spectroscopy and X-ray crystallography have been very successful in revealing the structure of the copper-binding site [7–11], but do not give thermodynamic data and reveal only limited information about stoichiometries. It is also important to characterize the association properties of these proteins, as the process of copper transfer involves transient protein–protein interactions between chaperones and partner proteins [5,6], and the mechanisms by which these processes occur will depend on the aggregation state of the proteins. To date, Atx1 is the only copper chaperone protein of this type for which the solution aggregation state of the apo- and copper-bound forms has been clearly demonstrated (being monomeric in both) [7]. Thus further studies are required to determine the association states of copper chaperones in solution and the factors that are important in determining them.

We have studied CopZ from the bacterium *Bacillus subtilis*, a 69-amino-acid Atx1-like protein that is thought to function as a copper chaperone. We report spectroscopic, bioanalytical and biochemical studies which show that copper binds to CopZ as copper(I), and that this process is coupled to the association of protein molecules into dimers. The nature of the copper(I)–CopZ complex depends on the overall loading of the sample, and we describe three distinct forms, with different copper(I) stoichiometries. The presence of excess dithiothreitol (DTT) during loading prevents the formation of the CopZ dimer, consistent with the recently published NMR structure of copper(I)–CopZ loaded under these conditions [11]. We discuss the significance of the different forms of the copper(I)–CopZ complex in relation both to the mechanism of copper transfer and to other copper chaperones.

## EXPERIMENTAL

### Strains, growth media and genetic methods

*Escherichia coli* strain JM109 (Promega) was used for cloning and expression, and was grown at 37 °C in Luria–Bertani broth [12], or on LA plates consisting of Luria–Bertani broth with 1.25 % (w/v) agar. Ampicillin, where appropriate, was used at a concentration of 100 mg/l. Molecular genetics techniques were used as described by Sambrook et al. [12]. Plasmid DNA was isolated using Quantum Prep miniprep kits (Bio-Rad) or Qiagen midiprep kits (Qiagen). Chromosomal DNA from *B. subtilis* strain 1A1 (Bacillus Genetic Stock Center, Columbus, OH, U.S.A.) was isolated as described previously [13]. Enzymes

---

for DNA manipulation were purchased from Roche or Promega. DNA sequencing was carried out by MWG Biotech or using a BigDye Terminator kit (Applied Biosystems, Warrington, Cheshire, U.K.) according to the manufacturer's instructions together with an ABI Prism 377 DNA sequencer.

### Cloning and site-directed mutagenesis of *B. subtilis copZ* (*yvgY*)

Initially, an 866 bp fragment containing *copZ* (originally designated *yvgY*) and the gene directly upstream, *yvgZ*, was amplified by PCR, with primers 5′-TTCATCCAGAACATCCAGCAGC-GG and 5′-GAAATATCGCGCCTCCCTAAAGGC, using chromosomal DNA from *Bacillus subtilis* 1A1 as template and *Pfu* DNA polymerase (Promega). The product was ligated into *Sma*I-cut pUC18, generating pMKNC1. *copZ* was subcloned from pMKNC1 using PCR with primers 5′-TT<u>CATATG</u>GAA-CAAAAAACATTGC and 5′-C<u>GAATTC</u>TTGAATCACTTG-GCTACG, and pMKNC1 as template. The 226 bp fragment was ligated into *Sma*I-cut pBluescript, generating pMKNC4. The primers introduced an *Nde*I site at the *copZ* translational start site and an *Eco*RI site downstream of the stop site. The *Nde*I/*Eco*RI *copZ* fragment was ligated into pAlter-Ex1 (Promega) containing a functional ampicillin resistance marker and cut with the same enzymes, generating pMKNC6. The *copZ* gene was confirmed by sequencing.

pMKNC6 was used to generate a mutated form of *copZ*, encoding the substitutions Cys-13 → Ser and Cys-16 → Ser, by site-directed mutagenesis, using a QuikChange mutagenesis kit (Stratagene) in accordance with the manufacturer's instructions. The mutagenic primer 5′-GGAATGTCTTCTCAGCACTCCG-TCAAAGCAG and its reverse complement were used to generate the mutations, which were confirmed by sequencing, giving pMKNC11.

### Purification of wild-type CopZ and Cys13Ser/Cys16Ser CopZ

In pMKNC6 and pMKNC11, expression of the *copZ* gene is under the control of the inducible *tac* promoter. Typically, 2 litres ($8 \times 250$ ml) of Luria–Bertani medium was inoculated with $8 \times 1.25$ ml of an overnight culture of *E. coli* JM109 containing the appropriate plasmid, and incubated at 37 °C, 200 rev./min until the $A_{600}$ was $\sim 0.2$. Isopropyl $\beta$-D-thiogalactoside was then added to a final concentration of 0.4 mM and the cultures were incubated with shaking for a further 4.5 h. Cells were harvested by centrifugation at 5000 $\mathbf{g}$ for 20 min at 4 °C and resuspended in 0.1 culture volume of 100 mM Hepes, pH 7.0. Lysozyme (Sigma) was added to a final concentration of 0.1 mg/ml and the cells were incubated at 30 °C for 15 min with gentle shaking. DNase and RNase (Sigma) were added to final concentrations of 10 $\mu$g/ml and 1 $\mu$g/ml respectively, and the cells were sonicated for $2 \times 8$ min 20 s using a Status US200 ultrasonicator (Novara) in pulse mode (0.2 s per s) set at 50 % power, while on ice. The lysate was centrifuged at 39 000 $\mathbf{g}$ for 20 min at 4 °C and the supernatant was heated slowly to 75 °C, stirred continuously for 15 min and placed on ice for a further 15 min. The suspension was centrifuged at 39 000 $\mathbf{g}$ for 20 min at 4 °C. DTT (Melford Laboratories Ltd., Ipswich, U.K.) was added to the supernatant to a final concentration of 15 mM, and the solution was passed through a 0.45 $\mu$m filter (Sartorius) before loading on to a 115 ml DEAE anion-exchange column (Amersham Biosciences), previously equilibrated with 300 ml of 100 mM Hepes, pH 7.0, and 15 mM DTT. A 1.2 litre gradient of 0–1 M NaCl in the same buffer was applied, with CopZ eluting at approx. 300 mM NaCl. CopZ-containing fractions (as determined by SDS/PAGE analysis) were concentrated to $< 5$ ml using an ultrafiltration cell

fitted with a YM3 membrane (Amicon; Millipore) operating at a pressure of 379.5 kPa (55 lbf/in²). The filtered protein solution was applied to a 130 ml Sephacryl S-100 gel filtration column, previously equilibrated with 350 ml of 100 mM Hepes, pH 7.0, 100 mM NaCl and 15 mM DTT. CopZ-containing fractions (as determined by SDS/PAGE) were concentrated as before and desalted using a G25 Sephadex column (PD-10; Amersham Biosciences) into 100 mM Hepes, pH 7.0. Buffer exchanges were carried out using an ultrafiltration cell, as described above, or a G25 Sephadex column.

The purity of preparations was assessed by SDS/PAGE analysis, which showed a single band consistent with the expected size of CopZ (results not shown), and electrospray ionization MS, using a VG platform electrospray mass spectrometer. For this, approx. 20 pmol of protein was prepared in 20 $\mu$l of acetonitrile/water/formic acid (1:1:0.005, by vol.), and collected data were processed with the supplied Masslynx software. Horse heart myoglobin (16951.48 Da) was used as a calibrant. The molecular mass of the wild-type protein was 7336.9 Da, and that of Cys13Ser/Cys16Ser CopZ was 7304.9 Da, which compare well with the expected values of 7338.1 and 7306.0 Da respectively. From this we concluded that the protein was pure and that no post-translational modifications had occurred. For analysis of copper-bound forms of CopZ, approx. 20 pmol of the protein was prepared in 10 % or 25 % (v/v) methanol/25 mM ammonium acetate, pH 7. For a sample containing one copper atom per protein, a peak corresponding to copper(I)–CopZ was observed at 7397.9 Da (predicted molecular mass 7401.6 Da) in addition to the apo-protein peak. Similar data were obtained for 0.5 and 1.5 copper-loaded samples. Higher association states of the protein were not detected; however, these are difficult to detect, due to the nature of the ionization process. The concentration of CopZ was determined using a molar absorption coefficient at 276 nm of $\epsilon = 1450$ M$^{-1} \cdot$ cm$^{-1}$ for the reduced protein, determined by the Edelhoch method [14] and by the bicinchoninic acid (BCA) method [15]. This very low value reflects the presence of only one tyrosine residue (and no tryptophans) in the protein.

The metal ion contents of CopZ, both as isolated and following the addition of copper, were determined using an ICP-AE (inductively coupled atomic emission) spectrometer (Varian Vista), calibrated with metal ion atomic absorption standards diluted to appropriate concentrations. Copper contents were also assayed using a colorimetric method employing the copper(I) chelator BCA. This was carried out as described previously [16], except that trichloroacetic acid was not used to precipitate protein. Instead, 0.25 ml of 65 % nitric acid was added to 0.75 ml of a solution of CopZ in 100 mM Hepes, pH 7, in a Teflon cell, which was sealed and incubated overnight at 90 °C. Once cool, 0.45 ml of 5 M NaOH was added, and 0.5 ml of the neutralized solution was mixed with sodium ascorbate and BCA solutions as described. As isolated, the protein was found to contain less than 0.01 equivalent of copper, and no other metals at significant levels. Thus the protein, as isolated, was considered to be in an apo-form.

The copper-binding motif of CopZ contains the disulphide oxidoreductase sequence CXXC, and, therefore, has the potential to form both intra- and inter-molecular disulphide bonds. In order to analyse the oxidation state of the protein as isolated, the reactivity of the cysteine thiol groups of CopZ was analysed using Ellman's reagent, DTNB [5,5′-dithiobis-(2-nitrobenzoic acid)] [17]. This revealed approx. 1 reactive thiol per CopZ, as isolated. A similar analysis of CopZ following reduction by 15 mM DTT and removal of excess reductant using a desalting column gave 1.7 reactive thiols per protein. The latter value is

somewhat lower than that expected (i.e. 2 per protein), and it is not clear why we are unable to detect all thiols. Analysis of Cys13Ser/Cys16Ser CopZ confirmed that the variant protein does not contain reactive thiols.

### Addition of copper ions to CopZ

Additions of copper to CopZ were made using a microsyringe (Hamilton) in an anaerobic glovebox (Faircrest Engineering) in which the oxygen concentration was kept below 2 p.p.m., using deoxygenated copper ion solutions freshly prepared in AnalaR water. Copper was added in one of two ways. (1) As a solution of copper(I), prepared from analytical-grade copper(I) chloride (Sigma), in 0.1 M HCl/1 M NaCl under anaerobic conditions [18]. As a control, we verified that addition of the acid solution used to prepare the copper stock solution to the protein did not itself cause any spectral changes. (2) As a solution of copper(II) chloride (analytical grade; Sigma). For single-addition experiments, unbound copper was removed by passage of the sample down a G25 Sephadex column before further analysis. Prior to all metal ion single-addition and titration experiments, CopZ was treated with 15 mM DTT in an anaerobic glovebox and subsequently passed down a G25 Sephadex column to remove DTT.

### Spectroscopic methods

UV–visible absorbance spectra were recorded on a Perkin–Elmer $\lambda$800, $\lambda$35 or EZ201 spectrophotometer. For titrations carried out within an anaerobic glovebox, UV–visible spectra were recorded using a fibre-optic-linked Hewlett–Packard diode array spectrophotometer. CD spectra were recorded using a Jasco J-810 spectropolarimeter interfaced to a Pentium PC. CD intensity is expressed as $\Delta\epsilon$ in units of $M^{-1} \cdot cm^{-1}$, with reference to the concentration of the protein. CD spectra were recorded over a wavelength range of 250–400 nm at a scan speed of $100 \text{ nm} \cdot \text{min}^{-1}$, a band width of 2 nm and with a response time of 1 s. Titration experiments were conducted using a sample cuvette only, and samples were incubated for 5 min after metal ion addition before spectra were recorded. Data were corrected for dilution effects. Luminescence measurements recorded at 25 °C as emission spectra (excitation wavelength 295 nm) were made using a Perkin–Elmer LS55 luminescence spectrometer, with a 350 nm band-pass filter. EPR spectra were measured with an X-band spectrometer (Bruker ER200D with an EPS 3220 computer system) fitted with an ESR9 liquid helium flow cryostat (Oxford Instruments). Copper integrations were performed using 1 mM copper(II) EDTA as a standard.

### Analytical methods

Sedimentation equilibrium experiments were performed using a Beckman XL-I analytical ultracentrifuge in an AN50Ti rotor at 20 °C, in 12 mm charcoal-filled Epon double-sector cells with quartz windows. Protein samples were prepared and loaded into the cells under anaerobic conditions. Data were acquired at 280 nm using the absorption optics. The sample volume was 110 $\mu$l and the reference sector of the cell contained identical buffer (50 mM Mops, 100 mM NaCl, pH 7.5). Samples were spun at speeds ranging from 20000 to 38000 rev./min until equilibrium was reached, as judged by cessation of change in scans collected 4 h apart. Data were analysed using supplied Beckman software. The density of the buffer was taken as 1.006 g/ml, and the partial specific volume of CopZ was calculated by the method of Cohn and Edsall using the program SEDNTERP [19].

Analytical gel filtration was performed using a Superdex 75 column (23.5 ml; Amersham Biosciences), equilibrated in thoroughly deoxygenated buffers and operated at a flow rate of 0.8 ml/min. Samples were prepared under anaerobic conditions. Calibration was performed using Blue Dextran (2000 kDa), BSA (67 kDa), ovalbumin (43 kDa), chymotrypsinogen A (25 kDa), RNase A (13.7 kDa) and tryptophan (204 Da) as standards (all purchased from Sigma).

## RESULTS

### Cloning, purification and characterization of CopZ and Cys13Ser/Cys16Ser CopZ

Searches of the *B. subtilis* genome revealed the presence of a gene, *copZ* (*yvgY*), which encodes a putative copper chaperone directly upstream of a gene, *yvgX*, that encodes a putative copper-transporting P-type ATPase. In order to study the interaction of CopZ with copper, *copZ* was cloned into an *E. coli* expression vector and wild-type CopZ was overproduced and purified. A strategy using a fusion or tagged CopZ protein product was avoided because, even when the fusion/tag is cleaved off, additional non-native amino acid residues remain at the tagged terminus. In order to confirm the importance of the two cysteine residues in the copper-binding motif MXCXXC (where X is any amino acid), Cys-13 and Cys-16 were replaced with serine residues and the variant protein was purified.

### Gel filtration/copper analysis of copper binding to CopZ

Copper binding to CopZ was investigated using a gel filtration/copper analysis assay (Table 1). Copper(I) was added under anaerobic conditions in a single aliquot; non-bound or weakly bound copper was removed by gel filtration and protein-associated copper was determined. The data indicate an overall stoichiometry of greater than 1, as addition of 1.5 equivalents resulted in the detection of $\sim$ 1.35 copper(I) per protein after one

**Table 1   Analysis of copper binding to CopZ**

Values are the equivalents of copper remaining bound to wild-type CopZ and to Cys13Ser/Cys16Ser CopZ following a single passage of samples containing various additions of copper down a desalting column, as determined by atomic emission spectroscopy and/or colorimetric assay. Copper was added as copper(I) to proteins in 20 or 100 mM Hepes/100 mM NaCl, pH 7.5, or as copper(II) to proteins in 100 mM Hepes, pH 7.0. Initial protein concentrations were 50–70 $\mu$M.

| Protein sample | Copper addition | | |
| --- | --- | --- | --- |
| | Added as | Ions added per protein | Copper ions detected per protein after gel filtration |
| CopZ as prepared | — | — | < 0.01 |
| | Cu(I) | 0.5 | 0.52 ± 0.09 |
| | | 1.0 | 0.92 ± 0.03 |
| | | | 0.92 ± 0.02* |
| | | 1.5 | 1.34 ± 0.01 |
| | | | 1.22 ± 0.02* |
| CopZ as prepared + DTT | Cu(I) | 1.2 | 0.97 ± 0.05 |
| Cys13Ser/Cys16Ser CopZ as prepared | — | — | < 0.01 |
| | Cu(I) | 0.5 | 0.19 ± 0.01 |
| | | 1.0 | 0.28 ± 0.01 |
| | | 1.5 | 0.39 ± 0.01 |
| CopZ as prepared | Cu(II) | 1.0 | 0.46 ± 0.03 |

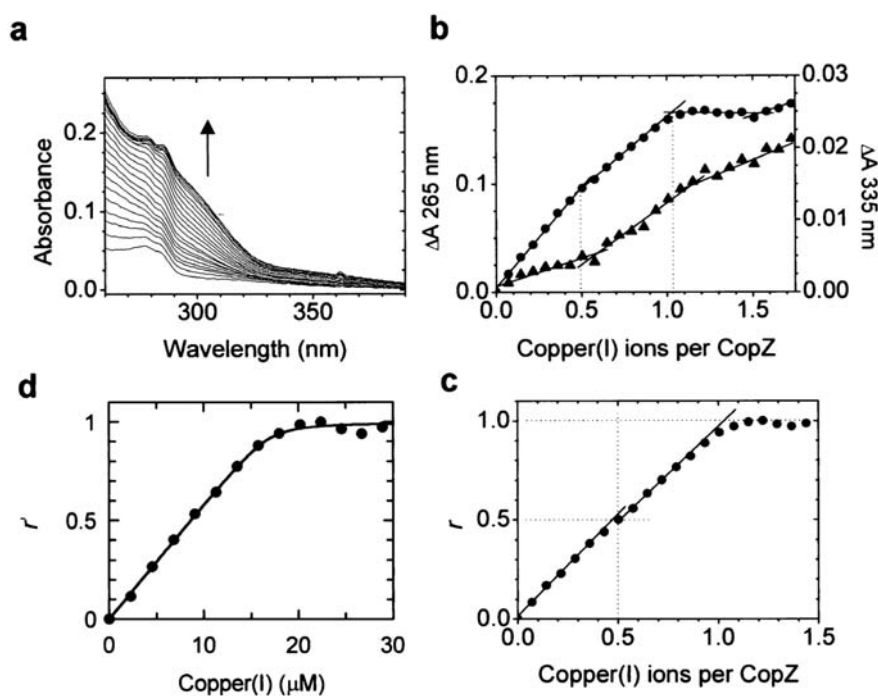\* Determined following a second gel filtration column pass.

**Figure 1 UV–visible absorbance titration of CopZ with copper(I)**

(**a**) Absorbance spectra of CopZ (33 $\mu$M) in 50 mM Mops buffer, pH 7.5, following the addition of 0–1.72 copper(I) ions per protein, added in aliquots of $\sim$ 0.07 equivalent. Pathlength, 1 cm; temperature, 25 °C. (**b**) Plots of absorbance changes at 265 nm ($\bullet$, left ordinate) and 335 nm ($\blacktriangle$, right ordinate) as a function of the number of copper(I) ions per CopZ. (**c**) Plot of fractional saturation, $r$, as a function of copper(I) per CopZ. For the calculation of $r$, additional weak binding observed at metal/protein stoichiometries $>$ 1.5 was ignored. Complications due to non-constant $\epsilon_{265}$ were overcome by first calculating fractional saturations for each tight binding phase (taking the break point in $\Delta A_{265}$ to represent saturating absorbance for form A) and then combining these to give overall saturation. (**d**) Plot of fractional saturation of the second tight binding phase, $r'$, as a function of copper(I) added beyond that required to saturate phase 1.

and $\sim$ 1.22 copper(I) per protein after two passes of the sample down a gel filtration column [no change was observed for loadings of 0.5 or 1 equivalent of copper(I) per protein following a second pass down a gel filtration column]. Addition of increasing levels of copper(I) to Cys13Ser/Cys16Ser CopZ gave low levels of bound copper, characteristic of weak binding to the variant protein. Addition of 1.2 equivalents of copper(I) to CopZ in the presence of DTT resulted in a binding stoichiometry of $\sim$ 1.

In order to investigate whether CopZ can bind copper(II), a similar experiment was performed with 1 equivalent of copper(II) chloride in place of the copper(I) salt. This resulted in binding of $\sim$ 0.5 copper per protein. The UV–visible spectrum of this sample (not shown) was indistinguishable in form from that resulting from the addition of copper(I), suggesting that the copper detected is actually present as copper(I). An EPR spectrum of this sample (not shown) revealed a characteristic $S = \frac{1}{2}$ copper(II) signal. However, double integration and comparison with a copper(II) standard showed that this accounted for $< 5\%$ of the copper present. We conclude that addition of copper(II) to CopZ results in bound copper(I). The source of electrons for the reduction is not clear, but partial autoreduction of protein redox cofactors is a well-known occurrence.

**UV–visible absorbance characterization of copper binding to CopZ**

Copper(I) binding to proteins via cysteine residues gives rise to cysteine-to-copper [ligand-to-metal (LM)] charge transfer (CT) transitions in the UV region of the spectrum [20,21], and so we

investigated copper(I) binding to CopZ under anaerobic conditions by UV–visible absorbance spectroscopy. As expected, intensity was observed in this region, becoming more intense as further copper(I) was added (Figure 1a). A plot of $\Delta A_{265}$ as a function of copper added (Figure 1b) has several interesting features. It reveals two clear phases of tight binding, which intersect at $\sim$ 0.5 and $\sim$ 1.0 copper(I) ion per protein respectively. The plot also indicates that additional, weak binding occurs at higher levels of copper. The form of the weak binding is unusual, in that all binding appears to be saturated at a level of $\sim$ 1 copper(I) per protein, and little or no additional intensity is observed until after $\sim$ 1.5 copper(I) per protein, where it begins to increase again. This effect was highly reproducible; essentially identical results were obtained for three separate titration experiments conducted on different occasions. A plot of $\Delta A_{335}$ as a function of copper added (Figure 1b) also reveals separate phases above and below 0.5 copper(I) per CopZ, indicating that the average optical properties of CopZ-bound copper are different above and below this stoichiometry. Increases in intensity are observed beyond a level of 1 per protein, consistent with binding beyond this stoichiometry.

We interpret the data in the range 0–1 copper(I) per protein in terms of the formation of two distinct forms of copper(I)-bound CopZ: form A is generated in the range 0–0.5 copper per protein, with $\epsilon_{265}$ and $\epsilon_{335}$ values of 5900 $\pm$ 200 and 250 $\pm$ 30 M$^{-1} \cdot$ cm$^{-1}$ respectively; while between 0.5 and 1.0 copper per protein, form A is converted into form B, with $\epsilon_{265}$ and $\epsilon_{335}$ values of 5300 $\pm$ 200 and 510 $\pm$ 50 M$^{-1} \cdot$ cm$^{-1}$ respectively. Studies of copper(I) binding to metallothioneins have shown that the molar absorption
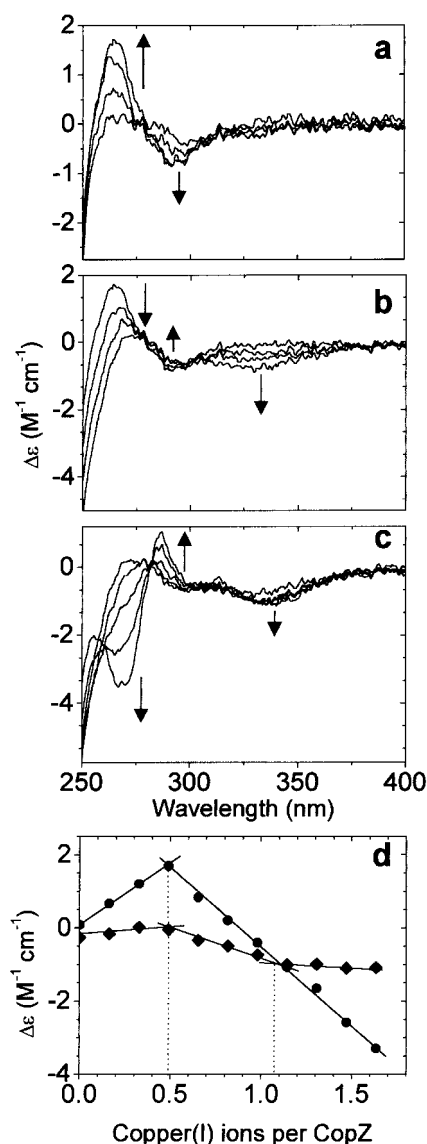
**Figure 2    CD titration of CopZ with copper(I)**

CD spectra were recorded following the addition of (**a**) 0–0.5 (0, 0.16, 0.32 and 0.48), (**b**) 0.5–1.0 (0.48, 0.63, 0.79 and 0.95) and (**c**) 1.0–1.6 (0.95, 1.10, 1.27, 1.42 and 1.58) copper(I) ions per CopZ. CopZ (30 $\mu$M) was in 50 mM Mops, pH 7.5. Pathlength, 1 cm; temperature, 25 °C. (**d**) Plots of $\Delta\epsilon_{265}$ (●) and $\Delta\epsilon_{335}$ (◆) as a function of copper(I) ions per CopZ.

coefficient of absorbance in this spectral region quantitatively reflects the number of cysteine–copper(I) bonds in the metal–protein complex, with an average of between 5200 and 5500 $M^{-1} \cdot cm^{-1}$ per bond [20]. This relationship apparently does not hold for CopZ, for which there are likely to be at least two, and probably three or four, cysteine–copper(I) bonds.

Because the generation of form A is essentially complete before any conversion into form B takes place, we conclude that the $K_d$ for the formation of form A is significantly lower than that for the subsequent generation of form B. In order to obtain estimates of the relevant $K_d$ values, we analysed data at 265 nm in terms of a binding curve, ignoring weak copper binding observed at > 1.5 copper(I) per CopZ. Figure 1(c) shows a plot of fractional saturation, $r$, as a function of copper(I) per CopZ

[up to 1.5 copper(I) per protein], which is similar in form to Figure 1(b) (in the range 0–1.5), but is much less obviously biphasic because differences in $\epsilon_{265}$ for the two forms are factored out in the calculation of $r$. We could not fit the first binding process (generation of form A), because the accuracy with which we can measure the concentration of bound copper (and therefore free copper) is not sufficient to characterize very tight binding. In addition, there are insufficient data reporting on the saturation characteristics of the first binding process. The second binding process (generation of form B) occurs with a significantly lower affinity and we are able to follow the saturation of this process. Thus we are able to fit these data (using a simple single site binding algorithm [22]) to obtain an estimate for the $K_d$. Figure 1(d) shows a plot of the second binding phase expressed as fractional saturation, $r'$ [where $r' = 0$ corresponds to all copper(I) present in form A and $r' = 1$ to all copper(I) in form B], as a function of copper(I) added after the formation of form A, with the fit drawn in. This gave a $K_d$ value of $\sim 1.2 \times 10^{-7}$ M and a stoichiometry of $0.54 \pm 0.01$ per protein. This value must be treated with caution, because the concentration of sites in the experiment was necessarily significantly higher than the estimated $K_d$. Nevertheless, the goodness of fit indicates that a $K_d$ value in the sub-micromolar range is a reasonable estimate.

Gel filtration/copper analysis showed that small but significant quantities of copper(I) bind to Cys13Ser/Cys16Ser CopZ (Table 1). This was investigated further by titrating the variant protein with copper(I) and following changes in UV–visible absorbance (results not shown). Gradual, small increases were observed in the UV region, which continued to increase in an essentially linear fashion, with no sign of saturation up to a level of 1.7 copper(I) per protein. The observed absorbance intensity most probably arises from LMCT transitions, although the identities of the ligands are unknown. This behaviour is characteristic of weak binding of copper(I), and is consistent with the metal-binding analysis data.

### CD spectroscopic characterization of copper binding to CopZ

CD spectroscopy has been frequently employed to monitor copper binding to proteins capable of assembling copper clusters, such as metallothioneins and related proteins [20,21,23]. Copper(I) additions were made to CopZ under anaerobic conditions and CD spectra were recorded. No major features are observed above 255 nm in the spectrum of the apo-protein, and so the observed multi-phasic CD response arises solely from copper(I) bound at chiral centres. Additions in the range 0–0.5 copper(I) ion per protein gave the spectra plotted in Figure 2(a). A derivative-like envelope develops, with a band at (+)265 nm, a less intense band at (−)287 nm and an isodichroic point at 280 nm. This is assigned to form A of copper(I)–CopZ, as identified by absorbance spectroscopy. Between 0.5 and 1.0 copper(I) per protein (Figure 2b), the intensity of the derivative feature is reduced and it shifts to (+)275 nm, while a weak band also develops at (−)335 nm, with a second isodichroic point at $\sim 300$ nm. These changes indicate the conversion of form A of copper(I)–CopZ into form B. Beyond a stoichiometry of 1, up to $\sim 1.6$ copper(I) per protein, further changes are observed (Figure 2c). A derivative-like feature develops, with a major band at (−)265 nm and a less intense band at $\sim$ (+)287 nm, with the isodichroic point maintained at 280 nm. The trends of these changes are shown clearly in plots of $\Delta\epsilon$ at 265 nm and 335 nm as a function of copper(I) added (Figure 2d).

Additions of copper(I) to Cys13Ser/Cys16Ser CopZ did not produce additional bands in the CD spectrum (results not shown),
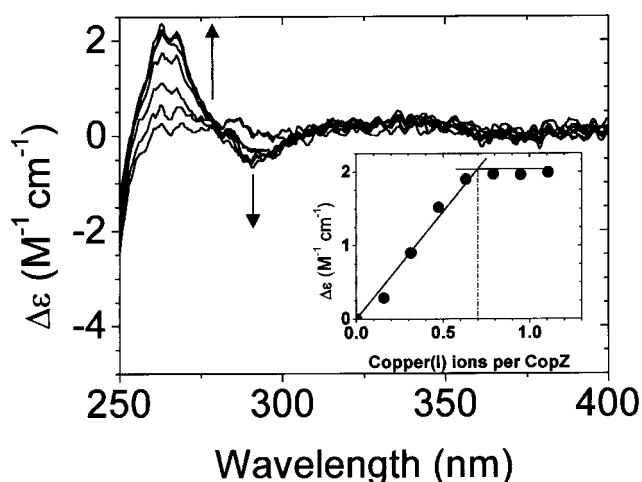
**Figure 3    CD titration of CopZ with copper(I) in the presence of DTT**

CD spectra were recorded following the addition of 0–1.1 (0.16, 0.32, 0.48, 0.63, 0.79, 0.95, 1.10) copper(I) ions per CopZ (30 $\mu$M) in 0.6 mM DTT and 50 mM Mops buffer, pH 7.5. Pathlength, 1 cm; temperature, 25 °C. The inset shows a plot of $\Delta\epsilon_{265}$ as a function of the number of copper(I) ions per CopZ.



**Figure 4    Analytical ultracentrifugation of apo-CopZ and copper-bound forms**

(**a**) Plots of apparent molecular mass ($M_w$) as a function of CopZ concentration for three samples of CopZ, at initial concentrations of 300 $\mu$M ($\square$), 150 $\mu$M ($\bigcirc$) and 75 $\mu$M ($\triangle$), in 50 mM Mops/100 mM NaCl, pH 7.5. (**b**) Plots of apparent molecular mass as a function of CopZ concentration, measured at 27 000 rev./min ($\square$), 32 000 rev./min ($\bigcirc$) and 38 000 rev./min ($\triangle$). The left, middle and right panels correspond to apo-CopZ (160 $\mu$M), CopZ containing 0.5 copper(I) ion per protein (50 $\mu$M) and CopZ containing 1 copper(I) per protein (50 $\mu$M) respectively. CopZ was in 50 mM Mops/100 mM NaCl, pH 7.5.

indicating that the small amount of copper shown to bind to the variant protein does not have an associated CD signal.

In order to place the copper(I)-binding properties of CopZ into context with the NMR structural study, CopZ was titrated under anaerobic conditions in the presence of a 20-fold excess of DTT, and CD spectra were recorded (Figure 3). Clearly, the presence of DTT significantly affects the copper(I)-binding properties of CopZ. A single phase is observed, consisting of a derivative feature very similar to that observed in phase 1 of the titration in the absence of DTT. However, binding saturation occurs at a stoichiometry of approx. 0.7 copper(I) ion per protein (inset of Figure 3).

### Luminescence characterization of copper binding to CopZ

Proteins that bind copper(I) ions in a solvent-shielded environment usually exhibit luminescence, with an emission band in the region of 600 nm [24]. We were unable to detect luminescence intensity in this region (at 25 °C) for any form of copper(I)–CopZ (results not shown), and we conclude that copper bound to CopZ is not solvent shielded.

### Analytical ultracentrifugation analysis of apo-CopZ and copper(I)-bound forms

The behaviour of CopZ in the presence of increasing concentrations of copper(I) indicated the likelihood that copper-mediated protein–protein associations may be involved. In order to investigate this further, association characteristics of apo- and copper(I)-loaded samples of CopZ were analysed by equilibrium sedimentation. Apo-CopZ was first analysed at a range of concentrations (300, 150 and 75 $\mu$M) at 20 000 rev./min. At each concentration, the data (absorbance at 280 nm as a function of radius) could be fitted to a single exponential, indicating that the protein behaves consistently as a homogeneous sample. Figure 4(a) shows plots of apparent molecular mass as a function of concentration, indicating that apo-CopZ has an apparent molecular mass of 10 200 $\pm$ 700 Da, a value significantly higher than
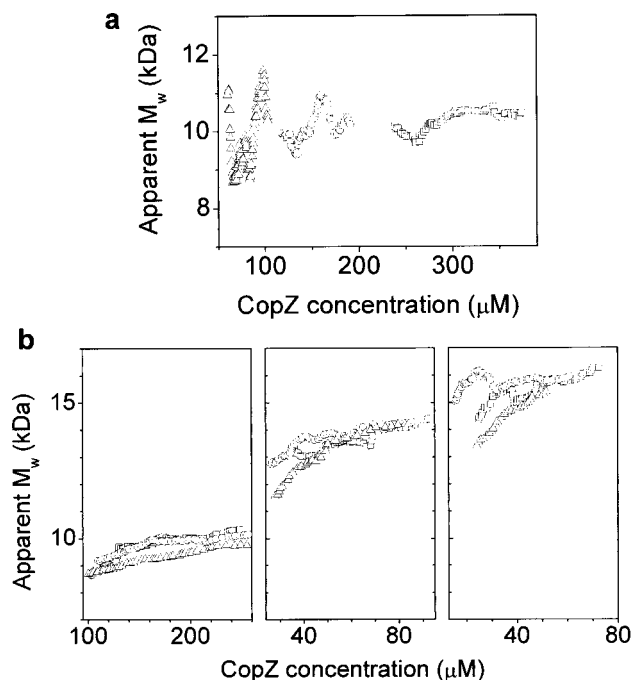
that expected for the CopZ monomer (7338 Da). CopZ samples containing 0, 0.5 and 1 copper(I) ion per protein were then analysed at 27 000, 32 000 and 38 000 rev./min respectively (Figure 4b). The behaviour of apo-CopZ was consistent with that of Figure 4(a), with an apparent molecular mass of 9650 $\pm$ 500 Da. Significant changes in the behaviour of CopZ occurred on binding of copper(I). At a loading of 0.5, the apparent molecular mass increased to 13 670 $\pm$ 650 Da, while at 1 copper(I) per protein the apparent molecular mass was 15 300 $\pm$ 1000 Da. The last two molecular-mass values are close to what would be expected for a CopZ dimer species (14 676 Da). The apparent molecular mass of apo-CopZ is significantly lower than these values, and we conclude that in the absence of copper(I) the protein is a monomer, as reported previously [11]. The fact that the apparent molecular mass is higher than expected could be due to the presence of a small component of higher-molecular-mass forms (e.g. dimers), although absorbance versus radius data fitted well to single exponentials. The inherent technical difficulties in establishing the molecular mass of small proteins with very low $\epsilon_{280}$ values may also be a contributory factor.

### Analytical gel filtration analysis of apo-CopZ and copper(I)-bound forms

To investigate further the association characteristics of apo-CopZ and copper(I)-loaded samples of CopZ, analytical gel filtration analysis was performed in the absence and presence of DTT. The chromatograms (relative $A_{280}$ intensity plotted as a
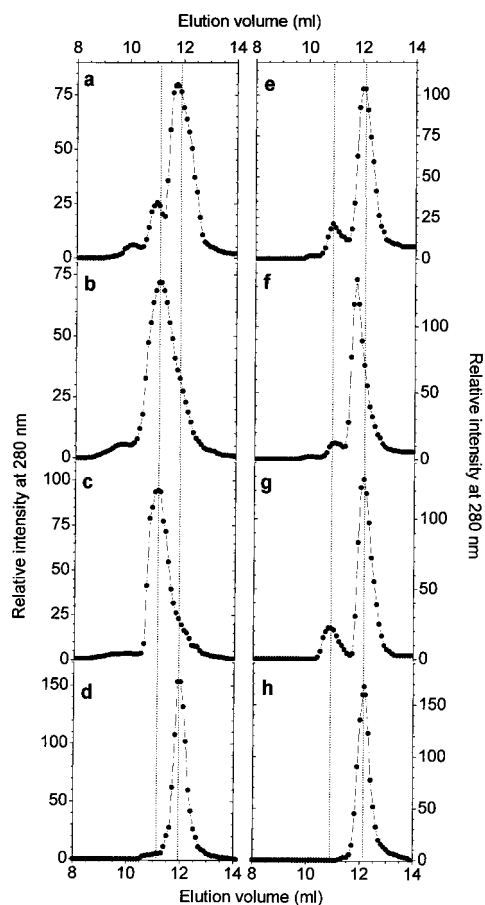
**Figure 5    Analytical gel filtration of apo-CopZ and copper-bound forms**

Plots showing relative $A_{280}$ intensity (arbitrary units) as a function of elution volume. Samples of CopZ ($\sim 300 \mu$M) were in 50 mM Mops/100 mM NaCl, pH 7.5, with (**a**) no added copper, (**b**) 0.5 copper(I) ion per protein or (**c**) 1 copper per protein. (**d**) Cys13Ser/Cys16Ser CopZ was in 50 mM Mops/100 mM NaCl, pH 7.5, with no added copper. Panels (**e**)–(**h**) are the same as (**a**)–(**d**) respectively, except that samples and equilibration/elution buffer contained 2.4 mM DTT.

function of elution volume) in Figures 5(a)–5(d) were measured in the absence of DTT. The trace for apo-CopZ (Figure 5a) contained a major peak at 11.9 ml (lower-molecular-mass species), with a minor peak at 11.1 ml (higher-molecular-mass species). An additional, very minor, peak was also detected at 10.0 ml. When CopZ was loaded with 0.5 copper(I) per protein, corresponding to the formation of form A of copper(I)–CopZ, the higher-molecular-mass species at 11.1 ml was the major component, with a shoulder at 11.9 ml indicating a minor amount of the lower-molecular-mass species (Figure 5b). At a level of 1 copper(I) per protein, corresponding to formation of form B, virtually all of the protein was present as the higher-molecular-mass species (Figure 5c). Analysis of Cys13Ser/Cys16Ser CopZ [without addition of copper(I)] (Figure 5d) revealed the presence of only the lower-molecular-mass species, which runs fractionally slower (elution volume of 12.0 ml) than the wild-type protein.

The chromatograms of Figures 5(e)–5(g) correspond to CopZ in the presence of DTT. Peaks at 10.9 and 12.1 ml correspond to the higher- and lower-molecular-mass species respectively. These are slightly shifted compared with those in the absence of DTT. Apo-CopZ (Figure 5e) was present mostly as the lower-

molecular-mass component, but with a minor amount of the higher-molecular-mass species remaining. At a loading of 0.5 copper(I) per CopZ (Figure 5f), the major species was eluted at 11.8 ml, corresponding to a molecular mass between the higher- and lower-molecular-mass species, but closer to the latter. At 1 copper(I) per protein (Figure 5g), CopZ was present mostly as the lower-molecular-mass species. Cys13Ser/Cys16Ser CopZ [without added copper(I)] gave only the lower-molecular-mass species (Figure 5h).

Reference to the calibration profile of the column indicated that all species have molecular-mass values between 22 and 28 kDa, suggesting that the protein exists in various oligomeric forms. However, because the hydrodynamic properties of proteins vary considerably, gel filtration is not a very reliable method for determining molecular mass. Therefore the molecular-mass values determined by equilibrium sedimentation analysis are considered to be more reliable. However, analytical gel filtration is useful for determining speciation, and we assign the lower- and higher-molecular-mass species to monomer and dimer forms of the protein respectively, and interpret these data in terms of a CopZ monomer–dimer equilibrium that is dependent on copper loading. In the absence of copper, essentially all of the protein is present as a monomer, both in the absence and in the presence of DTT (consistent with the NMR solution structure of apo-CopZ [11]). There is a small component of dimer, which could be due to the presence of some oxidized, disulphide-bonded proteins, although this remains in the presence of DTT. There is also a very minor component of an even higher-molecular-mass species, which could be a more extensively aggregated form of the protein. This is almost completely absent in the presence of DTT. Whatever their precise origins, the presence of small components of higher-molecular-mass forms of CopZ, which persist to varying extents in the presence of DTT, is consistent with the detection of approx. 1.7 reactive thiols per protein immediately after reduction (see Experimental). Cys13Ser/Cys16Ser CopZ is present only as a monomer in both the absence and the presence of DTT, consistent with its inability to form disulphide bonds.

In the absence of DTT and at a loading of 0.5 copper(I) per protein, CopZ exists mostly in the form of a dimer species, and it remains as a dimer at a loading of 1 copper(I) per protein. In the presence of DTT and at a loading of 0.5 copper(I) per CopZ, however, the protein is eluted at a point between the dimer and monomer species, suggesting that these two forms of the protein may be in rapid equilibrium as part of a complex reaction scheme involving DTT in equilibrium as a copper ligand. The protein is eluted at a position closer to that of the monomer, suggesting that this form is the major species. At a loading of 1 copper per protein, the monomer is the major species, and this is now well resolved from the dimer species, indicating that the rate of exchange for the equilibrium reaction is much lower than at a loading of 0.5.

## DISCUSSION

Elucidating the solution-state forms of copper chaperones is a key requirement for understanding the processes of copper binding and transfer. Although a great deal is known about the three-dimensional structures of copper chaperone proteins [7–11], less is known about the solution forms of these proteins. The exception to this is yeast Atx1, which NMR studies have shown to be a monomer in both its apo- and copper-bound forms [7]. For other Atx1-like proteins the situation is less clear. The crystal structure of copper(I)–Hah1, the human copper chaperone associated with the Menkes and Wilson P-type
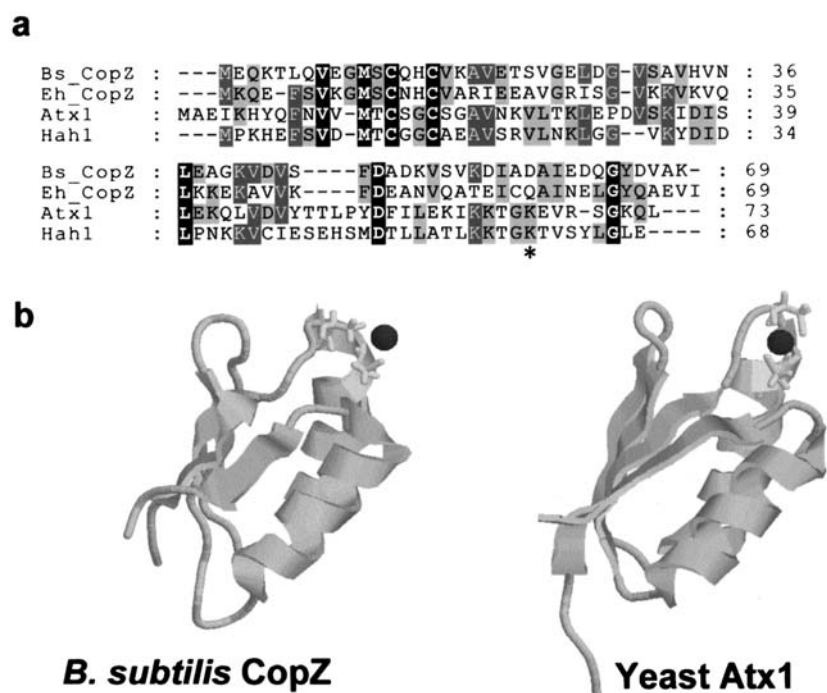
**Figure 6　Sequence and structural comparison of CopZ with known copper chaperones**

(**a**) Amino acid sequence alignment of *B. subtilis* CopZ (O32221) with CopZ from *Enterococcus hirae* (Q47840), yeast Atx1 (P38638) and human Hah1 (O00244), where the numbers in parentheses are the respective Swiss-Prot numbers (www.expasy.ch/sprot/). Numbers to the right of the figure indicate the amino acid number relative to the start of each polypeptide sequence. The asterisk indicates the position of Lys-65 in Atx1 and Hah1. The alignment was performed using the ClustalW program [33] and edited using the Genedoc program [34]. (**b**) Comparison of the NMR structures of the copper(I)-bound forms of *B. subtilis* CopZ and yeast Atx1. The structures are available at the Protein Data Bank (www.rcsb.org/pdb/) [35] under PDB numbers 1K0V (CopZ) and 1FD8 (Atx1). The figures were generated using the program Raswin (v2.6) [36].

ATPase copper transporters, revealed a dimeric structure, with the copper(I) at the protein–protein interface [10]. While this could be the solution form of the copper(I)-bound protein, the authors pointed out that it could be an artefact of crystallization. Copper-mediated dimerization may occur in *Enterococcus hirae* CopZ (*Eh*CopZ), which shares 38 % identity with *B. subtilis* CopZ [9] (Figure 6a). The NMR structure of the copper(I)-bound form of *Eh*CopZ could not be determined, due to the loss of signals from residues at the copper-binding site, which was proposed to be due to protein aggregation [9], and NMR rotational tumbling and dynamic light scattering measurements demonstrated self-aggregation of the protein upon copper(I) binding [9]. The exact nature of the aggregation was not demonstrated, although the formation of dimers was suggested. However, a recent EXAFS study of a 1:1 complex of copper(I) and *Eh*CopZ did not reveal a short copper–copper distance. Since dimerization is likely to be mediated by copper(I) binding, with the copper-binding sites of the monomers at the protein–protein interface (as in the Hah1 structure), this suggests that dimerization does not occur in this protein [28].

While our work was in progress, the NMR structure of *B. subtilis* CopZ was reported, indicating that the protein is a monomer in its apo- and copper-bound states [11]. The structure was determined for CopZ loaded with copper in the presence of excess DTT, and it was proposed that a DTT molecule, in addition to the two cysteine thiols, serves as a copper ligand. Our data confirm that apo-CopZ is monomeric and that addition of 1 copper(I) ion per CopZ in the presence of excess DTT results in mainly CopZ monomers with a single copper(I) bound (Figure

5g). However, data for copper binding to CopZ in the absence of DTT reveal very different behaviour. Under these conditions, CopZ exists in solution as a monomer (Figures 4a, 5a and 5e), but equilibrium sedimentation and gel filtration analyses show that addition of copper(I) causes the protein to associate into dimers (Figures 4b and 5b). This process is reflected in the spectroscopic characteristics of the metal–protein complex. LMCT bands observed in the UV region (Figure 1a) upon addition of copper increase in intensity (measured at 265 nm by absorbance and CD) in a linear fashion up to a loading of 0.5 copper(I) per protein, indicating the formation of form A of copper(I)–CopZ, in which copper very likely binds at the monomer interface, with ligation to the metal involving cysteine residues of the two monomers.

Additions of copper(I) at between 0.5 and 1.0 ion per CopZ do not alter the association state of the protein (i.e. the protein remains as a dimer) (Figures 4b and 5c), but do cause significant changes in both absorbance and CD spectra, indicating the conversion of form A of copper(I)–CopZ into form B. Absorbance spectra show that $\epsilon_{265}$ decreases (from 5900 to 5300 $M^{-1} \cdot cm^{-1}$) and $\epsilon_{335}$ increases (from 250 to 510 $M^{-1} \cdot cm^{-1}$), giving distinct phases in plots of $\Delta A_{265}$ and $\Delta A_{335}$ against copper(I) added (Figure 1b). Phase differences are more obvious in the CD spectra (Figures 2a, 2b and 2d), which show that binding of copper(I) beyond 0.5 per protein results in essentially the loss of the CD signal associated with binding of the first 0.5 copper(I) ion per protein (i.e. generation of form A). Thus the LMCT transitions of form B of copper(I)–CopZ do not give an overall CD signal at 265 nm, i.e. the LMCT transitions in form
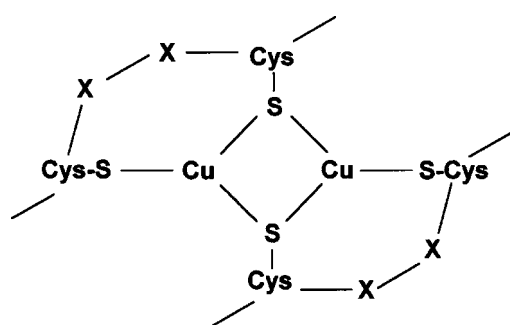
```
        X —— Cys
    X                  
 X             S       
                    
Cys-S —— Cu      Cu —— S-Cys
                    
               S        
                    X   
        Cys —— X
```

**Figure 7   Proposed structure of the copper centre of CopZ containing 1 equivalent of copper(I)**

Shown is a dimeric arrangement of CopZ monomers with two copper(I) ions bound at the monomer–monomer interface, each with ligands from both monomers.

B give rise to equal and opposite absorption of left and right circularly polarized light. Conversion of form A into form B is also characterized by the appearance of a CD band at $(-)335$ nm (Figures 2b and 2d). Intensity increases in the absorbance spectrum follow a similar pattern (Figure 1b), but the intensity of this band relative to the LMCT bands is significantly increased in CD. CD bands in this region are observed in metallothioneins containing multi-copper clusters, but are not observed in mononuclear copper(I) complexes such as $Cu(I)Cl_3^{2-}$ [25]. They are believed to arise from electric dipole forbidden, but magnetic dipole allowed, $3d \rightarrow 4s$ metal-cluster-centred transitions brought about by copper(I)–copper(I) interactions [20,21]. We conclude that form B of copper(I)–CopZ is a protein dimer containing a likely dinuclear copper(I) centre at the monomer–monomer interface. A possible structure for this centre features one cysteine residue from each monomer acting as a monodentate ligand to one copper, and the other acting as a bridging, bidentate ligand to both copper ions (Figure 7).

Further additions of copper(I) to CopZ containing 1 copper per protein result in additional binding, generating a further form of copper(I)–CopZ, form C. Copper-binding analysis showed that, following the addition of 1.5 copper(I) ions per protein, $\sim 1.35$ copper(I) ions per protein remained bound after gel filtration, and that the stoichiometry was still significantly greater than 1 after a second gel filtration pass (Table 1). An obvious possibility is that copper(I) binding beyond a level of 1 per protein is related to the weak binding of copper(I) observed for Cys13Ser/Cys16Ser CopZ. Several lines of evidence indicate that this is not the case. Firstly, copper(I) binding to the wild-type protein in the range 1–1.5 is significantly tighter than binding to the variant protein in the equivalent range 0–0.5 [copper-binding analysis showed that only $\sim 0.2$ copper(I) per protein remain bound; Table 1]. Secondly, additions of between 1 and 1.5 copper(I) ions per wild-type CopZ do not result in increased intensity at 265 nm in the absorbance spectrum (Figures 1a and 1b), whereas copper(I) binding to Cys13Ser/Cys16Ser CopZ does, indicating that these are different binding processes. Intensity increases similar to those observed for the variant protein are observed for the wild-type protein, but only above a loading of 1.5, suggesting that weak, probably non-specific, binding does occur, but as an additional process following the formation of form C. Thirdly, additions of between 1 and 1.5 copper(I) ions per wild-type CopZ cause significant changes in

the CD spectrum, particularly in the 265 nm region (Figure 2c). These changes cannot be due to additional LMCT intensity (because corresponding changes in the absorbance spectrum are not observed), and so we assign these changes to the direct interaction of the added copper with form B, leading to formation of form C. Interestingly, the CD spectrum observed at a level of $\sim 1.5$ copper(I) per protein is similar to that which would be expected if the CD responses in the UV region for the formation of forms A and B were of the same sign. Thus the additional copper interacts with the copper already bound, causing a modification of its absorption of left and right circularly polarized light. We conclude that copper(I) binding to CopZ at levels between 1 and 1.5 per protein is a specific process, generating a new form of copper(I)-bound CopZ, which may contain a trinuclear copper(I) centre. Polynuclear copper(I) centres occur in many proteins, including metallothioneins, copper-regulated transcription factors such as ACE1 (the transcriptional activator of the metallothionein gene in *Saccharomyces cerevisiae*), the copper chaperone Cox17, and in the N-terminal copper-binding domain of the Menkes protein [18,20,26,27]. Further studies are required to fully characterize form C of copper(I)–CopZ.

A question arising from this work is why CopZ exhibits such different behaviour in the absence and presence of DTT. Clearly, DTT is able to compete with cysteine thiols as ligands to copper. At a level of 1 copper per protein, DTT is able to out-compete cysteine residues from a second monomer, such that the majority of CopZ molecules are monomers. However, at levels of copper lower than 1 per CopZ, more complex mixtures of species are observed. Addition of copper up to 0.5 copper(I) ion per protein gave an equilibrium mixture of monomer and dimer species, again most likely involving DTT as a competing ligand for copper(I) (Figure 5f). Thus the inclusion of DTT results in an increased complexity in copper(I)-binding behaviour.

The copper-binding behaviour of CopZ (in the absence of DTT) may be an important feature of the function of this protein. Additions of copper(I) up to a loading of 0.5 per protein (to generate form A) result in binding that is significantly tighter than subsequent binding (to produce form B). We could not obtain an estimate of $K_d$ for the formation of form A, but were able to estimate that the $K_d$ for the conversion of form A into form B is in the sub-micromolar range (Figure 2d). We expect that the $K_d$ for the formation of form A is significantly lower. The $K_d$ for the formation of form C has not been estimated (because it cannot be followed by absorbance spectroscopy), but it must be significantly higher than that for the formation of form B.

Copper binds to CopZ in its $+1$ oxidation state even when added as copper(II) in the absence of a reducing agent. The copper-binding site must have a considerable preference for copper(I) over copper(II), resulting in a high redox potential for the copper(II)/(I) couple. Added copper(II) acts as a strong oxidizing agent, and is itself reduced to the $+1$ state. This is consistent with the principles of the hard/soft acid/base theory, which predicts that soft cysteine thiol ligands have a preference for soft metals such as copper(I). The source of electrons for the reduction is unknown, though auto-oxidation/reduction processes are often observed during handling of metalloprotein samples. The observed stoichiometry of $\sim 0.5$ copper(I) per protein [i.e. formation of form A of copper(I)–CopZ] following addition of 1 copper(II) per protein is consistent with the observed order of binding affinities; the first 0.5 copper(I) ion per protein binds with the highest affinity and therefore is likely to have the highest redox potential [for the copper(II)/copper(I) couple]. The potential of copper in form B of copper(I)–CopZ is likely to be lower and may not be sufficient to drive further reduction of added copper(II); hence reduction stops when 0.5 copper(I) ion

is bound per protein. Further investigations of copper binding to CopZ following addition of copper(II) are required to test this proposal.

Copper exchange between chaperone and partner proteins is believed to occur through the formation of a transient protein–protein complex mediated by electrostatic and hydrogen-bonding interactions between complementary protein surfaces [5,29]. The nature of the partner protein(s) of CopZ is not yet known. Atx1-like chaperones such as CopZ are usually associated with a metal-transporting P-type ATPase (e.g. Atx1 with CCC2, *Eh*CopZ with CopA and CopB). The gene encoding CopZ is immediately upstream of a gene, *yvgX*, that encodes such a transporter. The NMR structure of the metal-binding N-terminal part of YvgX (named CopA) was recently published [30]. A comparison of CopZ and CopA electrostatic surface potentials showed that a negatively charged patch exists near the copper site of CopZ and a positively charged patch occurs at a similar position in the second metal-binding domain of CopA, leading to the proposal that these could be complementary interacting surfaces.

This raises the question of how CopZ forms a homodimer species, in which what appear to be non-complementary surfaces are juxtaposed. The structure of the Hah1 homodimer gives a strong indication of how such a structure might be stabilized [10]. Apparently non-complementary positively charged surfaces of Hah1 are stabilized by an extended hydrogen-bonding network and by the shared bound copper ion [10]. A CopZ dimer could be stabilized in a similar way. Exchange of one CopZ protein from the dimer for a partner protein to form a heterodimer could then reasonably allow transfer of copper between them. The additional stabilization provided by the likely electrostatic complementarity of the partner protein surfaces would enable it to compete with CopZ monomer. Copper-loading-dependent changes in binding affinities could also be important for the mechanism of transfer of copper to a partner protein. As copper loading increases, its affinity for CopZ is decreased and, at least in thermodynamic terms, its transfer to another protein is favoured. This might provide a means by which a cell could distinguish between high and normal levels of copper.

A final question arising from the present work is why CopZ dimerizes upon copper binding but Atx1 does not. Compared with the CopZ structure, the bound copper of Atx1 is in a much more buried position (Figure 6b). One possibility is that copper chaperones need to ensure that their copper ions are not exposed non-specifically to other cellular components. CopZ appears to achieve this by associating into dimers around the copper, whereas Atx1 achieves protection by binding copper into a much less exposed site. In the Atx1 structure, the side chain of Lys-65 is located very close to the metal ion. Lys-65 is not essential for the *in vivo* function of Atx1 [31] and is not conserved in *B. subtilis* and *Eh*CopZ proteins (Figure 6a) or in *Synechocystis* PCC 6803 Atx1 [32]. However, the charge properties of the residue in this position may be important in determining metal-binding behaviour [31], as it was found that a glutamate could not be tolerated at this position in Atx1. Interestingly, *B. subtilis* CopZ contains an aspartate residue at this position (Figure 6a). Substitutions of residues around the copper-binding site may provide further insight into the variability of association state and copper-binding properties exhibited by metallo-chaperones.

## REFERENCES

1   Fraústo da Silva, J. J. R. and Williams, R. J. P. (1991) Copper: extracytoplasmic oxidases and matrix formation. In The Biological Chemistry of the Elements, pp. 388–397, Oxford University Press, Oxford

2   Halliwell, B. and Gutteridge, J. M. (1990) Role of free radicals and catalytic metal ions in human disease: an overview. Methods Enzymol. **186**, 1–85

3   Pufahl, R. A., Singer, C. P., Peariso, K. L., Lin, S.-J., Schmidt, P. J., Fahrni, C. J., Cizewski Culotta, V., Penner-Hahn, J. E. and O'Halloran, T. V. (1997) Metal ion chaperone function of the soluble Cu(I) receptor Atx1. Science **278**, 853–856

4   Labbé, S. and Thiele, D. J. (1999) Pipes and wiring: the regulation of copper uptake and distribution in yeast. Trends Microbiol. **7**, 500–505

5   Rosenzweig, A. C. and O'Halloran, T. V. (2000) Structure and chemistry of the copper chaperone proteins. Curr. Opin. Chem. Biol. **4**, 140–147

6   Harrison, M. D., Jones, C. E. and Dameron, T. (1999) Copper chaperones: function, structure and copper-binding properties. J. Biol. Inorg. Chem. **4**, 145–153

7   Arnesano, F., Banci, L., Bertini, I., Huffman, D. L. and O'Halloran, T. V. (2001) Solution structure of the Cu(I) and apo forms of the yeast metallochaperone, Atx1. Biochemistry **40**, 1528–1539

8   Rosenzweig, A. C., Huffman, D. L., Hou, M. Y., Wernimont, A. K., Pufahl, R. A. and O'Halloran, T. V. (1999) Crystal structure of the Atx1 metallochaperone protein at 1.02 Å resolution. Structure **7**, 605–617

9   Wimmer, R., Herrmann, T., Solioz, M. and Wüthrich, K. (1999) NMR structure and metal interactions of the CopZ copper chaperone. J. Biol. Chem. **274**, 22597–22603

10  Wernimont, A. K., Huffman, D. L., Lamb, A. L., O'Halloran, T. V. and Rosenzweig, A. C. (2000) Structural basis for copper transfer by the metallochaperone for the Menkes/Wilson diseases proteins. Nat. Struct. Biol. **7**, 766–771

11  Banci, L., Bertini, I., Del Conte, R., Markey, J. and Ruiz-Dueñas, F. J. (2001) Copper trafficking: the solution structure of *Bacillus subtilis* CopZ. Biochemistry **40**, 15660–15668

12  Sambrook, J., Fritsch, E. F. and Maniatis, T. (1989) Molecular Cloning: A Laboratory Manual, 2nd edn, Cold Spring Harbor Laboratory, Cold Spring Harbor, NY

13  Marmur, J. (1961) A procedure for the isolation of deoxyribonucleic acid from micro-organisms. J. Mol. Biol. **3**, 208–218

14  Pace, C. N., Vajdos, F., Fee, L., Grimsley, G. and Gray, T. (1995) How to measure and predict the molar absorption coefficient of a protein. Protein Sci. **4**, 2411–2423

15  Smith, P. K., Krohn, R. I., Hermanson, G. T., Mallia, A. K., Gartner, F. H., Provenzano, M. D., Fujimoto, E. K., Goeke, N. M., Olson, B. J. and Klenk, D. C. (1985) Measurement of protein using bicinchoninic acid. Anal. Biochem. **150**, 76–85

16  Baaghil, S., Thomson, A. J., Moore, G. R. and Le Brun, N. E. (2002) Studies of copper(II)-binding to bacterioferritin and its effect on iron(II) oxidation. J. Chem. Soc., Dalton Trans. 811–818

17  Riddles, P. W., Blakely, R. L. and Zemer, B. (1983) Reassessment of Ellman's reagent. Methods Enzymol. **91**, 49–60

18  Cobine, P. A., George, G. N., Winzor, D. J., Harrison, M. D., Mogahaddas, S. and Dameron, C. T. (2000) Stoichiometry of complex formation between copper(I) and the N-terminal domain of the Menkes protein. Biochemistry **39**, 6857–6863

19  Laue, T. M., Shah, B. D., Ridgeway, T. M. and Pelletier, S. L. (1992) Computer-aided interpretation of analytical sedimentation data for proteins. In The Analytical Ultracentrifuge in Biochemistry and Polymer Science (Harding, S. E., Rowe, A. J. and Horton, J., eds.), pp. 90–125, Royal Society of Chemistry, Cambridge

20  Pountney, D. L., Schauwecker, I., Zarn, J. and Vašák, M. (1994) Formation of mammalian $Cu_8$-metallothionein *in vitro*: evidence for the existence of two $Cu(I)_4$-thiolate clusters. Biochemistry **33**, 9699–9705

21  Hasler, D. W., Faller, P. and Vašák, M. (1998) Metal-thiolate clusters in the C-terminal domain of human neuronal growth inhibitory factor (GIF). Biochemistry **37**, 14966–14973

22  Keech, A. M., Le Brun, N. E., Wilson, M. T., Andrews, S. C., Moore, G. R. and Thomson, A. J. (1997) Spectroscopic studies of cobalt(II) binding to *Escherichia coli* bacterioferritin. J. Biol. Chem. **272**, 422–429

23  Bofill, R., Palacios, O., Capdevila, M., Cols, N., González-Duarte, R., Atrian, S. and González-Duarte, P. (1999) A new insight into the $Ag^+$ and $Cu^+$ binding sites in the metallothionein $\beta$ domain. J. Inorg. Biochem. **73**, 57–64

24  Stillman, M. J. and Gasyna, Z. (1991) Luminescence spectroscopy of metallothioneins. Methods Enzymol. **205**, 540–555

25  Stevenson, K. L., Braun, J. L., Davis, D. D., Kurtz, K. S. and Sparks, I. R. (1988) Luminescence and ultraviolet photoinduced electron-transfer in chlorocuprate(I) complexes in aqueous solution at room temperature. Inorg. Chem. **42**, 3472–3476

26  Dameron, C. T., Winge, D. R., George, G. N., Sansone, M., Hu, S. and Hamer, D. (1991) A copper-thiolate polynuclear cluster in the ACE1 transcription factor. Proc. Natl. Acad. Sci. U.S.A. **88**, 6127–6131

27  Heaton, D. N., George, G. N., Garrison, G. and Winge, D. R. (2001) The mitochondrial copper metallochaperone Cox17 exists as an oligomeric, polycopper complex. Biochemistry **40**, 743–751

28  Cobine, P. A., George, G. N., Jones, C. E., Wickramasinghe, W. A., Solioz, M. and Dameron, C. T. (2002) Copper transfer from the Cu(I) chaperone, CopZ, to the repressor, Zn(II)CopY: metal coordination environments and protein interactions. Biochemistry **41**, 5822–5829

29  Banci, L., Bertini, I., Ciofi-Baffoni, S., D'Onofrio, M., Gonnelli, L., Marhuenda-Egea, F. C. and Ruiz-Dueñas, J. (2002) Solution structure of the N-terminal domain of a potential copper-translocating P-type ATPase from *Bacillus subtilis* in the apo and Cu(I) loaded states. J. Mol. Biol. **317**, 415–429

30  Arnesano, F., Banci, L., Bertini, I., Cantini, F., Ciofi-Baffoni, S., Huffman, D. L. and O'Halloran, T. V. (2001) Characterization of the binding interface between the copper chaperone Atx1 and the first cytosolic domain of Ccc2 ATPase. J. Biol. Chem. **276**, 41365–41376

31  Portnoy, M. E., Rosenzweig, A. C., Rae, T., Huffman, D. L., O'Halloran, T. V. and Culotta, V. C. (1999) Structure-function analyses of the Atx1 metallochaperone. J. Biol. Chem. **274**, 15041–15045

32  Tottey, S., Rondet, S. A., Borrelly, G. P., Robinson, P. J., Rich, P. R. and Robinson, N. J. (2002) A copper metallochaperone for photosynthesis and respiration reveals metal-specific targets, interaction with an importer, and alternative sites for copper acquisition. J. Biol. Chem. **277**, 5490–5497

33  Thompson, J. D., Higgins, D. G. and Gibson, T. J. (1994) CLUSTAL W: improving the sensitivity of progressive multiple sequence alignment through sequence weighting, position-specific gap penalties and weight matrix choice. Nucleic Acids Res. **22**, 4673–4680

34  Nicholas, K. B. and Nicholas, Jr, H. B. (1997) GeneDoc: Analysis and Visualization of Genetic Variation (distributed by the authors; http://www.psc.edu/biomed/genedoc/)

35  Berman, H. M., Westbrook, J., Feng, Z., Gilliland, G., Bhat, T. N., Weissig, H., Shindyalov, I. N. and Bourne, P. E. (2000) The Protein Data Bank. Nucleic Acids Res. **28**, 235–242

36  Sayle, R. A. and Milner-White, E. J. (1995) RASMOL: biomolecular graphics for all. Trends Biochem. Sci. **20**, 374–376